

Angular Analysis of the $B^+ \rightarrow K^{*+} \mu^+ \mu^-$ Decay

R. Aaij *et al.**
(LHCb Collaboration)



(Received 4 January 2021; accepted 11 March 2021; published 22 April 2021)

We present an angular analysis of the $B^+ \rightarrow K^{*+}(\rightarrow K_S^0 \pi^+) \mu^+ \mu^-$ decay using 9 fb^{-1} of pp collision data collected with the LHCb experiment. For the first time, the full set of CP -averaged angular observables is measured in intervals of the dimuon invariant mass squared. Local deviations from standard model predictions are observed, similar to those in previous LHCb analyses of the isospin-partner $B^0 \rightarrow K^{*0} \mu^+ \mu^-$ decay. The global tension is dependent on which effective couplings are considered and on the choice of theory nuisance parameters.

DOI: 10.1103/PhysRevLett.126.161802

Transitions between b quarks and s quarks with the emission of two charged leptons, $\ell^+ \ell^-$, only proceed through loop-level processes. Such decays are therefore sensitive to possible contributions from heavy mediators that are inaccessible to direct-production searches. Recent studies of $b \rightarrow s \ell^+ \ell^-$ branching fractions [1–5], angular distributions [1,4,6–13], and ratios of branching fractions between decays with different flavours of lepton pairs [14–18] show discrepancies with respect to the predictions of the standard model (SM). While these deviations can be consistently explained by the presence of contributions from additional vector or axial-vector currents [19–37], effects from uncertainties related to hadronic form factors or long-distance contributions cannot be ruled out [38–42].

The $B \rightarrow K^* \mu^+ \mu^-$ decay, where K^* denotes the $K^*(892)$ meson, has been the subject of extensive studies [7,12,43,44]. A large number of these decays are recorded at the LHC experiments and the flavor of the B meson can be identified from the $K^* \rightarrow K \pi$ decay products. This allows the full set of angular observables of the $B \rightarrow K^* \mu^+ \mu^-$ decay to be studied. A recent study [12] of the $B^0 \rightarrow K^{*0} \mu^+ \mu^-$ decay channel by the LHCb Collaboration confirmed the tension in the angular observables with respect to the SM predictions.

This Letter reports the first measurement of the complete set of angular observables in the isospin partner decay $B^+ \rightarrow K^{*+} \mu^+ \mu^-$, with the K^{*+} meson reconstructed through the decay chain $K^{*+} \rightarrow K_S^0 \pi^+$ with $K_S^0 \rightarrow \pi^+ \pi^-$. Charge-conjugation is implied throughout this Letter. This decay is mediated by the same underlying processes as the

$B^0 \rightarrow K^{*0} \mu^+ \mu^-$ decay, while potentially receiving additional contributions from $\bar{b} \rightarrow \bar{u} W^+$ transitions, leading to the emission of a K^{*+} meson [45]. Furthermore, any deviation from isospin symmetry, as reported previously in the $B \rightarrow K^* \gamma$ decay [46], could result in a difference in the angular distributions between the isospin partners. In the SM, however, isospin-breaking effects are expected to be small. The analysis uses the dataset collected by the LHCb Collaboration in the years 2011, 2012 (run 1) and 2015–2018 (run 2), at center-of-mass energies of 7, 8, and 13 TeV, respectively. The dataset corresponds to an integrated luminosity of 9 fb^{-1} .

The LHCb detector [47,48] is a single-arm forward spectrometer covering the pseudorapidity range $2 < \eta < 5$, designed for the study of particles containing b or c quarks. The detector includes a high-precision tracking system consisting of a silicon-strip vertex detector surrounding the pp interaction region [49], a large-area silicon-strip detector located upstream of a dipole magnet with a bending power of about 4 Tm, and three stations of silicon-strip detectors and straw drift tubes [50,51] placed downstream of the magnet. The tracking system provides a measurement of the momentum p of charged particles with a relative uncertainty that varies from 0.5% at low momentum to 1.0% at 200 GeV/ c . The minimum distance of a track to a primary pp collision vertex (PV), the impact parameter, is measured with a resolution of $(15 + 29/p_T) \mu\text{m}$, where p_T is the component of the momentum transverse to the beam, in GeV/ c . Different types of charged hadrons are distinguished using information from two ring-imaging Cherenkov detectors [52]. Photons, electrons, and hadrons are identified by a calorimeter system consisting of scintillating-pad and pre-shower detectors, an electromagnetic and a hadronic calorimeter. Muons are identified by a system composed of alternating layers of iron and multiwire proportional chambers [53]. The online event selection is performed by a trigger [54,55], which consists of a hardware stage, based

*Full author list given at end of the Letter.

Published by the American Physical Society under the terms of the Creative Commons Attribution 4.0 International license. Further distribution of this work must maintain attribution to the author(s) and the published article's title, journal citation, and DOI. Funded by SCOAP³.

on information from the calorimeter and muon systems, followed by a software stage, which applies a full event reconstruction.

Simulated decays are used to model the effects of the reconstruction and the candidate selection. In the simulation, pp collisions are generated using PYTHIA [56] with a specific LHCb configuration [57]. Decays of unstable particles are described by EVTGEN [58], in which final-state radiation is generated using PHOTOS [59]. The interaction of the generated particles with the detector, and its response, are implemented using the GEANT4 toolkit [60], as described in Ref. [61]. Corrections to the simulation are applied to account for mismodeling in the p_T spectrum of the B^+ mesons and the multiplicity of tracks in the event. The corrections are obtained from a background-subtracted data sample of $B^+ \rightarrow (J/\psi \rightarrow \mu^+\mu^-)K^{*+}$ decays.

In the first two stages of the trigger, the event is selected based on kinematical and geometrical properties of the muons. In the last trigger stage, dimuon or topological trigger algorithms are used to select the B^+ candidate. The $K_S^0 \rightarrow \pi^+\pi^-$ decays are reconstructed in two different categories: the *long* category involves short-lived K_S^0 candidates for which the pions are reconstructed in the vertex detector; the *downstream* category comprises K_S^0 candidates that decay later, such that track segments of the pions can only be reconstructed in tracking detectors downstream of the vertex locator. The K_S^0 candidates reconstructed in the long category have better mass, momentum, and vertex resolution than those in the downstream category, where the latter has a larger sample size than the former. The K_S^0 candidates are required to have an invariant mass within 30 MeV/c^2 of the known K_S^0 mass [62].

The $K^{*+} \rightarrow K_S^0\pi^+$ decay is reconstructed by combining a K_S^0 candidate with a charged pion and requiring their invariant mass to be within 100 MeV/c^2 of the world average of the K^{*+} mass [62]. The $B^+ \rightarrow K^{*+}\mu^+\mu^-$ candidates are formed by combining the K^{*+} candidate with two well-identified, oppositely charged muons. The B^+ candidates are required to have an invariant mass, $m(K_S^0\pi^+\mu^+\mu^-)$, in the range 5150–6000 MeV/c^2 . The lower value of the mass window is chosen to reject background from partially reconstructed $B \rightarrow K_S^0\pi^+\pi^+\mu^-$ decays. Dimuon pairs having invariant mass squared q^2 around the $\phi(1020)$ ($0.98 < q^2 < 1.1 \text{ GeV}^2/c^4$), J/ψ ($8.0 < q^2 < 11.0 \text{ GeV}^2/c^4$), and $\psi(2S)$ ($12.5 < q^2 < 15.0 \text{ GeV}^2/c^4$) resonances are vetoed. All tracks in the final state are required to have a significant impact parameter with respect to any PV and the B^+ candidate decay vertex needs to be well displaced from any PV in the event. A kinematical fit [63] is performed to the full decay chain, in which the reconstructed K_S^0 mass is constrained to the known value [62].

Decays of B^0 mesons to the $K_S^0\mu^+\mu^-$ final state with a pion added can form a peaking structure in the B^+ mass

window. Therefore, candidates with an invariant mass $m(K_S^0\mu^+\mu^-)$ within 50 MeV/c^2 of the known B^0 mass are vetoed. Background originating from $B^+ \rightarrow (J/\psi \rightarrow \mu^+\mu^-)K^{*+}$ decays is probed by testing the $K_S^0\pi^+$ and dimuon invariant masses formed by exchanging the particle hypotheses between the pion from the K^{*+} meson decay and the muon with the same charge. The candidates with a dimuon mass within 50 MeV/c^2 of the J/ψ meson mass and a $K_S^0\pi^+$ invariant mass within 30 MeV/c^2 of the K^{*+} mass are then rejected. The background from B decays with two hadrons misidentified as muons is negligible.

To increase the signal-to-background ratio, a multivariate classification is employed. The data are split into four subsets, according to the run 1 and run 2 data-taking periods and the category of the K_S^0 meson. A boosted decision tree with gradient boosting [64,65] from the TMVA toolkit [66] is then trained on each dataset individually, using simulated events as a proxy for signal and candidates with $m(K_S^0\pi^+\mu^+\mu^-)$ larger than 5400 MeV/c^2 as a proxy for background. The variables include kinematical and topological properties of the final state or intermediate particles, the quality of the vertex of the B^+ candidate, and an isolation criterion related to the asymmetry in p_T between all tracks inside a cone around the flight directions of the B^+ candidates and the tracks associated to the B^+ decay products [67]. Figure 1 shows the B^+ -candidate invariant mass distribution $m(K_S^0\pi^+\mu^+\mu^-)$ for all the selected data. A fit model with a double-sided Crystal Ball function for the signal and an exponential function for the background component is overlaid. The number of $B^+ \rightarrow K^{*+}\mu^+\mu^-$ signal candidates from this fit is 737 ± 34 , where the uncertainty is statistical only.

Ignoring the natural width of the K^{*+} meson, the decay $B^+ \rightarrow K^{*+}\mu^+\mu^-$ can be fully described by four variables:

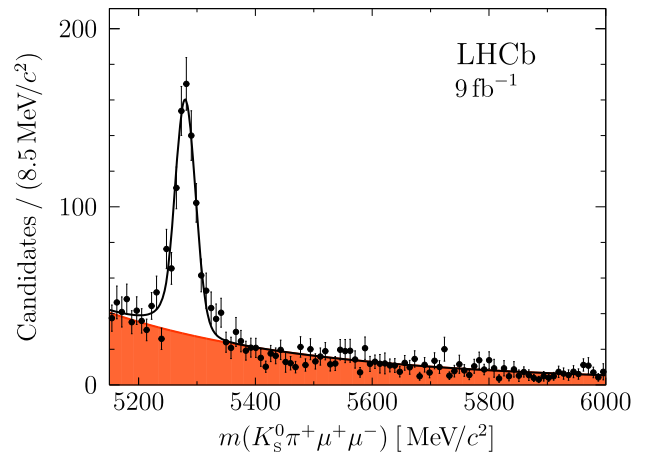


FIG. 1. Distribution of the $K_S^0\pi^+\mu^+\mu^-$ invariant mass. The black points represent the full dataset, while the solid curve shows the fit result. The background component is represented by the orange shaded area.

q^2 and the set of three angles $\vec{\Omega} = (\theta_\ell, \theta_K, \phi)$. The angle between the μ^+ (μ^-) and the direction opposite to that of the B^+ (B^-) in the rest frame of the dimuon system is denoted θ_ℓ . The angle between the direction of the K_S^0 and the B^+ (B^-) in the rest frame of the K^{*+} (K^{*-}) system is denoted θ_K . The angle ϕ is the angle between the plane defined by the momenta of the muon pair and the plane

defined by the kaon and pion momenta in the B^+ (B^-) rest frame. A full description of the angular basis is given in Ref. [44].

Averaging over B^+ and B^- decays, with rates, respectively, denoted Γ and $\bar{\Gamma}$, the differential decay rate of the $B^+ \rightarrow K^{*+} \mu^+ \mu^-$ decay with the $K_S^0 \pi^+$ system in a P -wave configuration is

$$\begin{aligned} \frac{1}{d(\Gamma + \bar{\Gamma})/dq^2} \frac{d^4(\Gamma + \bar{\Gamma})}{dq^2 d\vec{\Omega}} \Big|_P = & \frac{9}{32\pi} \left[\frac{3}{4}(1 - F_L) \sin^2 \theta_K + F_L \cos^2 \theta_K + \frac{1}{4}(1 - F_L) \sin^2 \theta_K \cos 2\theta_\ell \right. \\ & - F_L \cos^2 \theta_K \cos 2\theta_\ell + S_3 \sin^2 \theta_K \sin^2 \theta_\ell \cos 2\phi + S_4 \sin 2\theta_K \sin 2\theta_\ell \cos \phi + S_5 \sin 2\theta_K \sin \theta_\ell \cos \phi \\ & \left. + \frac{4}{3} A_{\text{FB}} \sin^2 \theta_K \cos \theta_\ell + S_7 \sin 2\theta_K \sin \theta_\ell \sin \phi + S_8 \sin 2\theta_K \sin 2\theta_\ell \sin \phi + S_9 \sin^2 \theta_K \sin^2 \theta_\ell \sin 2\phi \right], \end{aligned} \quad (1)$$

where F_L is the fraction of the longitudinally polarized K^{*+} mesons, A_{FB} is the forward-backward asymmetry of the dimuon system, and S_i are other CP -averaged observables [7].

The $K_S^0 \pi^+$ system can also be in an S -wave configuration, which modifies the differential decay rate to

$$\begin{aligned} \frac{1}{d(\Gamma + \bar{\Gamma})/dq^2} \frac{d^4(\Gamma + \bar{\Gamma})}{dq^2 d\vec{\Omega}} \Big|_{P+S} = & (1 - F_S) \frac{1}{d(\Gamma + \bar{\Gamma})/dq^2} \frac{d^4(\Gamma + \bar{\Gamma})}{dq^2 d\vec{\Omega}} \Big|_P + \frac{3}{16\pi} F_S \sin^2 \theta_l + \frac{9}{32\pi} (S_{11} + S_{13} \cos 2\theta_l) \cos \theta_K \\ & + \frac{9}{32\pi} (S_{14} \sin 2\theta_l + S_{15} \sin \theta_l) \sin \theta_K \cos \phi + \frac{9}{32\pi} (S_{16} \sin \theta_l + S_{17} \sin 2\theta_l) \sin \theta_K \sin \phi, \end{aligned} \quad (2)$$

where F_S denotes the S -wave fraction and the coefficients S_{11}, S_{13} – S_{17} arise from interference between the S - and P -wave amplitudes. Throughout this Letter, F_S and the interference coefficients are treated as nuisance parameters. In addition to the observable basis comprising F_L, A_{FB} and S_3 – S_9 , a basis with so-called optimized observables, denoted $P_i^{(o)}$, for which the leading form-factor uncertainties cancel [68], is used. The notation for the $P_i^{(o)}$ observables is defined in Ref. [43].

Due to the limited number of signal candidates, the observables cannot all be measured simultaneously. A folding procedure is therefore employed that uses symmetries of the differential decay rate in the angles to cancel some observables, reducing the number of free parameters in the fit. By performing different folds, all angular observables can be studied, without any loss in precision. Five different folds are used to study the observables A_{FB} and S_9 (P_2 and P_3), S_4 (P'_4), S_5 (P'_5), S_7 (P'_6), and S_8 (P'_8), respectively. The observables F_L and S_3 (P_1) are measured in each fold. This procedure is detailed in Ref. [69] and was previously used in Refs. [8–10, 43, 44]. The values of F_L and S_3 (P_1) are taken from the same fold that is used to extract the value of S_8 (P'_8), as the number of free parameters in the fit is the smallest in this fold.

The angular observables are extracted using an unbinned maximum-likelihood fit to the B^+ candidate mass and the three decay angles in intervals of q^2 . The eight narrow and two wide q^2 intervals are identical to those in Refs. [7, 12]. The angular distributions are fitted with the function described in Eq. (2) for the signal, and with second-order polynomials in $\cos \theta_K$ and $\cos \theta_\ell$ for the background. The background in the ϕ angle is uniform. No significant correlation is observed between the angular background distributions in the B^+ candidate mass sidebands, justifying a factorization of the background description in the three decay angles.

The reconstruction and selection efficiency varies over the angular and q^2 phase space. This acceptance effect is parametrized before folding using the sum over the product of four one-dimensional Legendre polynomials, each depending on one angle or q^2 . This is analogous to the procedure used in Ref. [12]. The effect is corrected using weights derived from simulation. The weight then corresponds to the inverse of the efficiency. No dependence of the acceptance effect on the K^{*+} candidate mass is observed.

Given the low signal yield and narrow q^2 intervals, the S -wave fraction F_S cannot be determined with sufficient

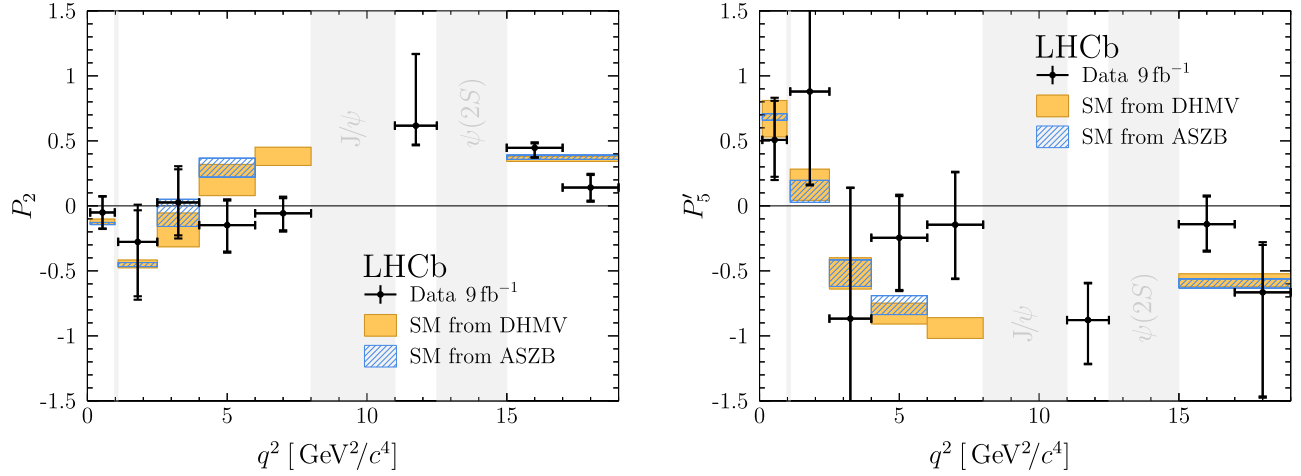


FIG. 2. The CP -averaged observables (left) P_2 and (right) P'_5 in intervals of q^2 . The first (second) error bars represent the statistical (total) uncertainties. The theoretical predictions in blue are based on Ref. [77] with hadronic form factors taken from Refs. [78–80] and are obtained with the FLAVIO software package [84] (version 2.0.0). The theoretical predictions in orange are based on Refs. [81,82] with hadronic form factors from Ref. [83]. The gray bands indicate the regions of excluded $\phi(1020)$, J/ψ , and $\psi(2S)$ resonances.

precision to guarantee unbiased results for the P -wave angular observables. Therefore, a two-dimensional unbinned maximum-likelihood fit to $m(K_S^0\pi^+\mu^+\mu^-)$ and the K^{*+} candidate mass $m(K_S^0\pi^+)$ is first performed in three q^2 intervals: 1.1–8.0, 11.0–12.5, and 15.0–19.0 GeV^2/c^4 . The $m(K_S^0\pi^+\mu^+\mu^-)$ distribution is fitted using the signal and background model described above. The K^{*+} candidate mass is fitted using a relativistic Breit-Wigner function to describe the P -wave component, the LASS parametrization to describe the S -wave component [70] and a linear function to describe the combinatorial background. S - and P -wave interference terms are neglected in this treatment. The value of F_S in the default narrow q^2 intervals is then computed by multiplying the value of F_S in the broad intervals with the ratio between F_L in the narrow and broad intervals. This procedure assumes a similar q^2 dependence of the longitudinal component of the P wave and the S wave and is broadly compatible with the results from Ref. [5]. Given the weak dependence of the P -wave observables on the value of F_S , this procedure ensures unbiased results without relying on values of F_S from an external measurement. Pseudoexperiments indicate that determining F_S in this manner induces at most a bias of 13% of the statistical uncertainty on the angular observables. This is treated as a systematic uncertainty. All values of F_S are measured to be positive and compatible with the results in Ref. [5].

Fitting the folded dataset only provides statistical correlations between observables measured in the same fold. In order to obtain the correlations between all observables, the bootstrapping technique [71] is used to produce a large number of pseudodatasets. The measurement of the observables in each fold of these pseudodatasets enables computing the correlations between observables in different folds. The statistical precision of the elements of the correlation

matrix is determined to be around 0.11. In order to ensure correct coverage in the presence of physical boundaries of the observables, the statistical uncertainty for each observable in each q^2 interval for the signal channel is evaluated using the Feldman-Cousins technique [72].

The full analysis procedure with acceptance correction, extraction of F_S , and extraction of the angular observables, is tested on a sample of $B^+ \rightarrow J/\psi K^{*+}$ decays with the same selection as applied to the signal channel, but requiring the dimuon invariant mass squared to be in the range 8.68–10.09 GeV^2/c^4 . The results are found to be in good agreement with previous measurements from the BABAR [73], Belle [74], and LHCb [75] experiments.

Several sources of systematic uncertainties are considered and their sizes are estimated using pseudoexperiments. Various contributions to the overall systematic uncertainty are related to the correction of acceptance effects. They include the limited size of the simulation sample and the parametrization of the acceptance function. Other systematic uncertainties are related to the correction of differences between data and simulation, the model of the B^+ candidate mass distribution and angular background, the impact of the $B^0 \rightarrow K_S^0\mu^+\mu^-$ veto on the mass distribution of the combinatorial background, the angular resolution, and the effect of constraining the value of F_S with a two-dimensional fit. Pseudoexperiments are used to assess a possible bias introduced by the fit procedure. The pseudodata samples are generated based on the result of the fit to data or on the predictions from either the SM or a new physics scenario favoured by the LHCb measurement from Ref. [12] with the real part of the Wilson coefficient C_9 shifted by -1 with respect to SM predictions. Here, C_9 is the strength of the vector coupling in an effective field theory of b quark to s quark transitions. The largest bias

observed is 33% of the statistical uncertainty for S_4 in the q^2 interval 4.0–6.0 GeV²/c⁴. Given that the biases can depend on the values of the observables themselves, the largest biases observed among the three pseudodata samples are taken as systematic uncertainties. The potential exchange of the π^+ mesons from the decays of the K^{*+} and K_S^0 candidates and the angular background description differing between the upper and lower mass sidebands are both considered as further sources of systematic uncertainty. Both effects are found to be negligible. All systematic uncertainties are added in quadrature and their total size is reported together with the numerical results of the observables in Table I and II of the Supplemental Material [76]. A summary of the contributions from the various sources is given in Table XXIII of the Supplemental Material [76]. The statistical uncertainty dominates for all q^2 intervals and all observables, which implies that correlations with the results from Ref. [12] are negligible.

The results of the angular fits for the observables $P_2 = \frac{2}{3}A_{\text{FB}}/(1 - F_L)$ and $P'_5 = S_5/\sqrt{F_L(1 - F_L)}$ are shown in Fig. 2. They are compared with the two SM predictions taken from Ref. [77] with hadronic form factors from Refs. [78–80], and from Refs. [81,82] with hadronic form factors from Ref. [83]. The rest of the observables are presented in Figs. 3 and 4 in the Supplemental Material to this Letter [76]. The numerical results of the angular fits to the data are presented in Tables I and II, where values for the two wide q^2 intervals are also given. The correlations are given in Tables III–XII and XIII–XXII for the S_i and $P_i^{(\prime)}$ observables, respectively.

The majority of observables show good agreement with the SM predictions, F_L and A_{FB} agree well with the measurements in Ref. [13]. The largest local discrepancy is in the measurement of P_2 in the 6.0–8.0 GeV²/c⁴ interval, where a deviation of 3.0σ with respect to the SM prediction is observed. The pattern of deviations from the SM predictions in the observables S_5 (P'_5) and A_{FB} (P_2) broadly agrees with the deviations observed in the $B^0 \rightarrow K^{*0}\mu^+\mu^-$ channel.

The FLAVIO package [84] (version 2.0.0) is used to perform a fit to the angular observables varying the parameter $\text{Re}(C_9)$, which is motivated by Refs. [7,12]. In order to minimize the theoretical uncertainties related to contributions from virtual charm-quark loops [83] and broad charmonium resonances [85–87], the narrow q^2 intervals up to 6.0 GeV²/c⁴ plus the wide q^2 interval $15.0 < q^2 < 19.0$ GeV²/c⁴ are included in the fit. The default FLAVIO SM nuisance parameters are used, including form-factor parameters and subleading corrections to account for long-distance QCD interference effects with the charmonium decay modes [77,78]. The best-fit point results in a shift with respect to the SM value of $\text{Re}(C_9)$ of -1.9 and gives a tension with the SM of 3.1σ . However, the tension observed depends on the q^2 intervals considered,

which effective couplings are varied and the handling of the SM nuisance parameters.

In summary, using the complete pp dataset collected with the LHCb experiment in runs 1 and 2, the full set of angular observables for the decay $B^+ \rightarrow K^{*+}\mu^+\mu^-$ is measured for the first time. The results confirm the global tension with respect to the SM predictions previously reported in the decay $B^0 \rightarrow K^{*0}\mu^+\mu^-$.

We express our gratitude to our colleagues in the CERN accelerator departments for the excellent performance of the LHC. We thank the technical and administrative staff at the LHCb institutes. We acknowledge support from CERN and from the national agencies: CAPES, CNPq, FAPERJ, and FINEP (Brazil); MOST and NSFC (China); CNRS/IN2P3 (France); BMBF, DFG, and MPG (Germany); INFN (Italy); NWO (Netherlands); MNiSW and NCN (Poland); MEN/IFA (Romania); MSHE (Russia); MICINN (Spain); SNSF and State Secretariat for Education, Research and Innovation (Switzerland); NASU (Ukraine); STFC (United Kingdom); DOE NP and NSF (USA). We acknowledge the computing resources that are provided by CERN, IN2P3 (France), KIT and DESY (Germany), INFN (Italy), SURF (Netherlands), PIC (Spain), GridPP (United Kingdom), RRCKI and Yandex LLC (Russia), CSCS (Switzerland), IFIN-HH (Romania), CBPF (Brazil), PL-GRID (Poland), and OSC (USA). We are indebted to the communities behind the multiple open-source software packages on which we depend. Individual groups or members have received support from AvH Foundation (Germany); EPLANET, Marie Skłodowska-Curie Actions, and ERC (European Union); A*MIDEX, ANR, Labex P2IO and OCEVU, and Région Auvergne-Rhône-Alpes (France); Key Research Program of Frontier Sciences of CAS, Chinese Academy of Sciences President's International Fellowship Initiative, CAS CCEPP, Fundamental Research Funds for the Central Universities, and Sci. & Tech. Program of Guangzhou (China); RFBR, RSF, and Yandex LLC (Russia); GVA, XuntaGal, and GENCAT (Spain); the Royal Society and the Leverhulme Trust (United Kingdom).

-
- [1] B. Aubert *et al.* (BABAR Collaboration), *Phys. Rev. D* **73**, 092001 (2006).
 - [2] R. Aaij *et al.* (LHCb Collaboration), *J. High Energy Phys.* **06** (2014) 133.
 - [3] R. Aaij *et al.* (LHCb Collaboration), *J. High Energy Phys.* **06** (2015) 115.
 - [4] R. Aaij *et al.* (LHCb Collaboration), *J. High Energy Phys.* **09** (2015) 179.
 - [5] R. Aaij *et al.* (LHCb Collaboration), *J. High Energy Phys.* **11** (2016) 047.
 - [6] T. Aaltonen *et al.* (CDF Collaboration), *Phys. Rev. Lett.* **108**, 081807 (2012).

- [7] R. Aaij *et al.* (LHCb Collaboration), *J. High Energy Phys.* **02** (2016) 104.
- [8] S. Wehle *et al.* (Belle Collaboration), *Phys. Rev. Lett.* **118**, 111801 (2017).
- [9] A. M. Sirunyan *et al.* (CMS Collaboration), *Phys. Lett. B* **781**, 517 (2018).
- [10] M. Aaboud *et al.* (ATLAS Collaboration), *J. High Energy Phys.* **10** (2018) 047.
- [11] R. Aaij *et al.* (LHCb Collaboration), *J. High Energy Phys.* **09** (2018) 146.
- [12] R. Aaij *et al.* (LHCb Collaboration), *Phys. Rev. Lett.* **125**, 011802 (2020).
- [13] A. M. Sirunyan *et al.* (CMS Collaboration), arXiv:2010.13968.
- [14] J. P. Lees *et al.* (BABAR Collaboration), *Phys. Rev. D* **86**, 032012 (2012).
- [15] R. Aaij *et al.* (LHCb Collaboration), *J. High Energy Phys.* **08** (2017) 055.
- [16] R. Aaij *et al.* (LHCb Collaboration), *Phys. Rev. Lett.* **122**, 191801 (2019).
- [17] S. Choudhury *et al.* (Belle Collaboration), arXiv:1908.01848.
- [18] S. Wehle *et al.* (Belle Collaboration), arXiv:1904.02440 [Phys. Rev. Lett. (to be published)].
- [19] W. Altmannshofer, S. Gori, M. Pospelov, and I. Yavin, *Phys. Rev. D* **89**, 095033 (2014).
- [20] G. Hiller and M. Schmaltz, *Phys. Rev. D* **90**, 054014 (2014).
- [21] B. Gripaios, M. Nardecchia, and S. A. Renner, *J. High Energy Phys.* **05** (2015) 006.
- [22] I. de Medeiros Varzielas and G. Hiller, *J. High Energy Phys.* **06** (2015) 072.
- [23] A. Crivellin, G. D’Ambrosio, and J. Heeck, *Phys. Rev. Lett.* **114**, 151801 (2015).
- [24] A. Celis, J. Fuentes-Martín, M. Jung, and H. Serôdio, *Phys. Rev. D* **92**, 015007 (2015).
- [25] A. Falkowski, M. Nardecchia, and R. Ziegler, *J. High Energy Phys.* **11** (2015) 173.
- [26] R. Barbieri, C. W. Murphy, and F. Senia, *Eur. Phys. J. C* **77**, 8 (2017).
- [27] A. Crivellin, D. Müller, and T. Ota, *J. High Energy Phys.* **09** (2017) 040.
- [28] F. Sala and D. M. Straub, *Phys. Lett. B* **774**, 205 (2017).
- [29] P. Ko, Y. Omura, Y. Shigekami, and C. Yu, *Phys. Rev. D* **95**, 115040 (2017).
- [30] J.-H. Sheng, R.-M. Wang, and Y.-D. Yang, *Int. J. Theor. Phys.* **58**, 480 (2019).
- [31] G. Hiller, D. Loose, and I. Nišandžić, *Phys. Rev. D* **97**, 075004 (2018).
- [32] M. Algueró, B. Capdevila, A. Crivellin, S. Descotes-Genon, P. Masjuan, J. Matias, and J. Virto, *Eur. Phys. J. C* **79**, 714 (2019).
- [33] J. Aebischer, W. Altmannshofer, D. Guadagnoli, M. Reboud, P. Stangl, and D. M. Straub, *Eur. Phys. J. C* **80**, 252 (2020).
- [34] A. Arbey, T. Hurth, F. Mahmoudi, D. Martinez Santos, and S. Neshatpour, *Phys. Rev. D* **100**, 015045 (2019).
- [35] M. Ciuchini, A. M. Coutinho, M. Fedele, E. Franco, A. Paul, L. Silvestrini, and M. Valli, *Eur. Phys. J. C* **79**, 719 (2019).
- [36] K. Kowalska, D. Kumar, and E. M. Sessolo, *Eur. Phys. J. C* **79**, 840 (2019).
- [37] A. K. Alok, A. Dighe, S. Gangal, and D. Kumar, *J. High Energy Phys.* **06** (2019) 089.
- [38] S. Jäger and J. Martin Camalich, *Phys. Rev. D* **93**, 014028 (2016).
- [39] J. Lyon and R. Zwicky, arXiv:1406.0566.
- [40] M. Ciuchini, M. Fedele, E. Franco, S. Mishima, A. Paul, L. Silvestrini, and M. Valli, *J. High Energy Phys.* **06** (2016) 116.
- [41] C. Bobeth, M. Chrzaszcz, D. van Dyk, and J. Virto, *Eur. Phys. J. C* **78**, 451 (2018).
- [42] N. Gubernari, D. van Dyk, and J. Virto, *J. High Energy Phys.* **02** (2021) 088.
- [43] R. Aaij *et al.* (LHCb Collaboration), *Phys. Rev. Lett.* **111**, 191801 (2013).
- [44] R. Aaij *et al.* (LHCb Collaboration), *J. High Energy Phys.* **08** (2013) 131.
- [45] P. Ball, G. W. Jones, and R. Zwicky, *Phys. Rev. D* **75**, 054004 (2007).
- [46] T. Horiguchi *et al.* (Belle Collaboration), *Phys. Rev. Lett.* **119**, 191802 (2017).
- [47] A. A. Alves, Jr. *et al.* (LHCb Collaboration), *J. Instrum.* **3**, S08005 (2008).
- [48] R. Aaij *et al.* (LHCb Collaboration), *Int. J. Mod. Phys. A* **30**, 1530022 (2015).
- [49] R. Aaij *et al.*, *J. Instrum.* **9**, P09007 (2014).
- [50] R. Arink *et al.*, *J. Instrum.* **9**, P01002 (2014).
- [51] P. d’Argent *et al.*, *J. Instrum.* **12**, P11016 (2017).
- [52] M. Adinolfi *et al.*, *Eur. Phys. J. C* **73**, 2431 (2013).
- [53] A. A. Alves, Jr. *et al.*, *J. Instrum.* **8**, P02022 (2013).
- [54] R. Aaij *et al.*, *J. Instrum.* **8**, P04022 (2013).
- [55] R. Aaij *et al.*, *J. Instrum.* **14**, P04013 (2019).
- [56] T. Sjöstrand, S. Mrenna, and P. Skands, *Comput. Phys. Commun.* **178**, 852 (2008); *J. High Energy Phys.* **05** (2006) 026.
- [57] I. Belyaev *et al.*, *J. Phys. Conf. Ser.* **331**, 032047 (2011).
- [58] D. J. Lange, *Nucl. Instrum. Methods Phys. Res., Sect. A* **462**, 152 (2001).
- [59] P. Golonka and Z. Was, *Eur. Phys. J. C* **45**, 97 (2006).
- [60] J. Allison, K. Amako, J. Apostolakis, H. Araujo, P. Dubois *et al.* (Geant4 Collaboration), *IEEE Trans. Nucl. Sci.* **53**, 270 (2006); S. Agostinelli *et al.* (Geant4 Collaboration), *Nucl. Instrum. Methods Phys. Res., Sect. A* **506**, 250 (2003).
- [61] M. Clemencic, G. Corti, S. Easo, C. R. Jones, S. Miglioranza, M. Pappagallo, and P. Robbe, *J. Phys. Conf. Ser.* **331**, 032023 (2011).
- [62] P. Zyla *et al.* (Particle Data Group), *Prog. Theor. Exp. Phys.* **2020**, 083C01 (2020).
- [63] W. D. Hulsbergen, *Nucl. Instrum. Methods Phys. Res., Sect. A* **552**, 566 (2005).
- [64] L. Breiman, J. H. Friedman, R. A. Olshen, and C. J. Stone, *Classification and Regression Trees* (Wadsworth International Group, Belmont, California, USA, 1984).
- [65] Y. Freund and R. E. Schapire, *J. Comput. Syst. Sci.* **55**, 119 (1997).
- [66] H. Voss, A. Hoecker, J. Stelzer, and F. Tegenfeldt, *Proc. Sci. ACAT2007* (2007) 040.
- [67] R. Aaij *et al.* (LHCb Collaboration), *Eur. Phys. J. C* **79**, 537 (2019).
- [68] S. Descotes-Genon, J. Matias, M. Ramon, and J. Virto, *J. High Energy Phys.* **01** (2013) 048.
- [69] M. De Cian, Ph.D. thesis, University of Zurich, Report No. CERN-THESIS-2013-145, 2013, <https://cds.cern.ch/record/1605179>.

- [70] D. Aston *et al.*, *Nucl. Phys.* **B296**, 493 (1988).
 [71] B. Efron, *Ann. Stat.* **7**, 1 (1979).
 [72] G. J. Feldman and R. D. Cousins, *Phys. Rev. D* **57**, 3873 (1998).
 [73] B. Aubert *et al.* (BABAR Collaboration), *Phys. Rev. D* **76**, 031102 (2007).
 [74] R. Itoh *et al.* (Belle Collaboration), *Phys. Rev. Lett.* **95**, 091601 (2005).
 [75] R. Aaij *et al.* (LHCb Collaboration), *Phys. Rev. D* **88**, 052002 (2013).
 [76] See Supplemental Material at <http://link.aps.org/supplemental/10.1103/PhysRevLett.126.161802> for fit projections, tabular and graphical displays of the results with correlation matrices and a summary of systematic uncertainties.
 [77] W. Altmannshofer and D. M. Straub, *Eur. Phys. J. C* **75**, 382 (2015).
 [78] A. Bharucha, D. M. Straub, and R. Zwicky, *J. High Energy Phys.* **08** (2016) 098.
 [79] R. R. Horgan, Z. Liu, S. Meinel, and M. Wingate, *Phys. Rev. D* **89**, 094501 (2014).
 [80] R. Horgan, Z. Liu, S. Meinel, and M. Wingate, *Proc. Sci. LATTICE2014* (2015) 372.
 [81] S. Descotes-Genon, L. Hofer, J. Matias, and J. Virto, *J. High Energy Phys.* **06** (2016) 092.
 [82] B. Capdevila, A. Crivellin, S. Descotes-Genon, J. Matias, and J. Virto, *J. High Energy Phys.* **01** (2018) 093.
 [83] A. Khodjamirian, T. Mannel, A. A. Pivovarov, and Y. M. Wang, *J. High Energy Phys.* **09** (2010) 089.
 [84] D. M. Straub, *arXiv:1810.08132*.
 [85] B. Grinstein and D. Pirjol, *Phys. Rev. D* **70**, 114005 (2004).
 [86] M. Beylich, G. Buchalla, and T. Feldmann, *Eur. Phys. J. C* **71**, 1635 (2011).
 [87] S. Braß, G. Hiller, and I. Nisandzic, *Eur. Phys. J. C* **77**, 16 (2017).

R. Aaij,³² C. Abellán Beteta,⁵⁰ T. Ackernley,⁶⁰ B. Adeva,⁴⁶ M. Adinolfi,⁵⁴ H. Afsharnia,⁹ C. A. Aidala,⁸⁵ S. Aiola,²⁶ Z. Ajaltouni,⁹ S. Akar,⁶⁵ J. Albrecht,¹⁵ F. Alessio,⁴⁸ M. Alexander,⁵⁹ A. Alfonso Alberro,⁴⁵ Z. Aliouche,⁶² G. Alkhazov,³⁸ P. Alvarez Cartelle,⁵⁵ S. Amato,² Y. Amhis,¹¹ L. An,⁴⁸ L. Anderlini,²² A. Andreianov,³⁸ M. Andreotti,²¹ F. Archilli,¹⁷ A. Artamonov,⁴⁴ M. Artuso,⁶⁸ K. Arzymatov,⁴² E. Aslanides,¹⁰ M. Atzeni,⁵⁰ B. Audurier,¹² S. Bachmann,¹⁷ M. Bachmayer,⁴⁹ J. J. Back,⁵⁶ S. Baker,⁶¹ P. Baladron Rodriguez,⁴⁶ V. Balagura,¹² W. Baldini,²¹ J. Baptista Leite,¹ R. J. Barlow,⁶² S. Barsuk,¹¹ W. Barter,⁶¹ M. Bartolini,^{24,h} F. Baryshnikov,⁸¹ J. M. Basels,¹⁴ G. Bassi,²⁹ B. Batsukh,⁶⁸ A. Battig,¹⁵ A. Bay,⁴⁹ M. Becker,¹⁵ F. Bedeschi,²⁹ I. Bediaga,¹ A. Beiter,⁶⁸ V. Belavin,⁴² S. Belin,²⁷ V. Bellee,⁴⁹ K. Belous,⁴⁴ I. Belov,⁴⁰ I. Belyaev,³⁹ G. Bencivenni,²³ E. Ben-Haim,¹³ A. Berezhnoy,⁴⁰ R. Bernet,⁵⁰ D. Berninghoff,¹⁷ H. C. Bernstein,⁶⁸ C. Bertella,⁴⁸ A. Bertolin,²⁸ C. Betancourt,⁵⁰ F. Betti,^{20,d} I. A. Bezshyiko,⁵⁰ S. Bhasin,⁵⁴ J. Bhom,³⁴ L. Bian,⁷³ M. S. Bieker,¹⁵ S. Bifani,⁵³ P. Billoir,¹³ M. Birch,⁶¹ F. C. R. Bishop,⁵⁵ A. Bizzeti,^{22,r} M. Björn,⁶³ M. P. Blago,⁴⁸ T. Blake,⁵⁶ F. Blanc,⁴⁹ S. Blusk,⁶⁸ D. Bobulska,⁵⁹ J. A. Boelhauve,¹⁵ O. Boente Garcia,⁴⁶ T. Boettcher,⁶⁴ A. Boldyrev,⁸² A. Bondar,⁴³ N. Bondar,³⁸ S. Borghi,⁶² M. Borisyak,⁴² M. Borsato,¹⁷ J. T. Borsuk,³⁴ S. A. Bouchiba,⁴⁹ T. J. V. Bowcock,⁶⁰ A. Boyer,⁴⁸ C. Bozzi,²¹ M. J. Bradley,⁶¹ S. Braun,⁶⁶ A. Brea Rodriguez,⁴⁶ M. Brodski,⁴⁸ J. Brodzicka,³⁴ A. Brossa Gonzalo,⁵⁶ D. Brundu,²⁷ A. Buonauro,⁵⁰ C. Burr,⁴⁸ A. Bursche,²⁷ A. Butkevich,⁴¹ J. S. Butter,³² J. Buytaert,⁴⁸ W. Byczynski,⁴⁸ S. Cadettu,²⁷ H. Cai,⁷³ R. Calabrese,^{21,f} L. Calefice,^{15,13} L. Calero Diaz,²³ S. Cali,²³ R. Calladine,⁵³ M. Calvi,^{25,i} M. Calvo Gomez,⁸⁴ P. Camargo Magalhaes,⁵⁴ A. Camboni,⁴⁵ P. Campana,²³ A. F. Campoverde Quezada,⁵ S. Capelli,^{25,i} L. Capriotti,^{20,d} A. Carbone,^{20,d} G. Carboni,³⁰ R. Cardinale,^{24,h} A. Cardini,²⁷ I. Carli,⁶ P. Carniti,^{25,i} K. Carvalho Akiba,³² A. Casais Vidal,⁴⁶ G. Casse,⁶⁰ M. Cattaneo,⁴⁸ G. Cavallero,⁴⁸ S. Celani,⁴⁹ J. Cerasoli,¹⁰ A. J. Chadwick,⁶⁰ M. G. Chapman,⁵⁴ M. Charles,¹³ Ph. Charpentier,⁴⁸ G. Chatzikonstantinidis,⁵³ C. A. Chavez Barajas,⁶⁰ M. Chefdeville,⁸ C. Chen,³ S. Chen,²⁷ A. Chernov,³⁴ S.-G. Chitic,⁴⁸ V. Chobanova,⁴⁶ S. Cholak,⁴⁹ M. Chrzaszcz,³⁴ A. Chubykin,³⁸ V. Chulikov,³⁸ P. Ciambone,²³ M. F. Cicala,⁵⁶ X. Cid Vidal,⁴⁶ G. Ciezarek,⁴⁸ P. E. L. Clarke,⁵⁸ M. Clemencic,⁴⁸ H. V. Cliff,⁵⁵ J. Closier,⁴⁸ J. L. Cobbedick,⁶² V. Coco,⁴⁸ J. A. B. Coelho,¹¹ J. Cogan,¹⁰ E. Cogneras,⁹ L. Cojocariu,³⁷ P. Collins,⁴⁸ T. Colombo,⁴⁸ L. Congedo,^{19,c} A. Contu,²⁷ N. Cooke,⁵³ G. Coombs,⁵⁹ G. Corti,⁴⁸ C. M. Costa Sobral,⁵⁶ B. Couturier,⁴⁸ D. C. Craik,⁶⁴ J. Crkovská,⁶⁷ M. Cruz Torres,¹ R. Currie,⁵⁸ C. L. Da Silva,⁶⁷ E. Dall'Occo,¹⁵ J. Dalseno,⁴⁶ C. D'Ambrosio,⁴⁸ A. Danilina,³⁹ P. d'Argent,⁴⁸ A. Davis,⁶² O. De Aguiar Francisco,⁶² K. De Bruyn,⁷⁸ S. De Capua,⁶² M. De Cian,⁴⁹ J. M. De Miranda,¹ L. De Paula,² M. De Serio,^{19,c} D. De Simone,⁵⁰ P. De Simone,²³ J. A. de Vries,⁷⁹ C. T. Dean,⁶⁷ W. Dean,⁸⁵ D. Decamp,⁸ L. Del Buono,¹³ B. Delaney,⁵⁵ H.-P. Dembinski,¹⁵ A. Dendek,³⁵ V. Denysenko,⁵⁰ D. Derkach,⁸² O. Deschamps,⁹ F. Desse,¹¹ F. Dettori,^{27,e} B. Dey,⁷³ P. Di Nezza,²³ S. Didenko,⁸¹ L. Dieste Maronas,⁴⁶ H. Dijkstra,⁴⁸ V. Dobishuk,⁵² A. M. Donohoe,¹⁸ F. Dordei,²⁷ A. C. dos Reis,¹ L. Douglas,⁵⁹ A. Dovbnya,⁵¹ A. G. Downes,⁸ K. Dreimanis,⁶⁰ M. W. Dudek,³⁴ L. Dufour,⁴⁸ V. Duk,⁷⁷ P. Durante,⁴⁸ J. M. Durham,⁶⁷ D. Dutta,⁶² M. Dziewiecki,¹⁷ A. Dziurda,³⁴ A. Dzyuba,³⁸ S. Easo,⁵⁷ U. Egede,⁶⁹ V. Egorychev,³⁹ S. Eidelman,^{43,u} S. Eisenhardt,⁵⁸ S. Ek-In,⁴⁹ L. Eklund,^{59,v} S. Ely,⁶⁸ A. Ene,³⁷ E. Epple,⁶⁷ S. Escher,¹⁴ J. Eschle,⁵⁰ S. Esen,³² T. Evans,⁴⁸ A. Falabella,²⁰ J. Fan,³ Y. Fan,⁵ B. Fang,⁷³ N. Farley,⁵³ S. Farry,⁶⁰ D. Fazzini,^{25,i} P. Fedin,³⁹ M. Féo,⁴⁸ P. Fernandez Declara,⁴⁸ A. Fernandez Prieto,⁴⁶ J. M. Fernandez-tenllado Arribas,⁴⁵ F. Ferrari,^{20,d}

L. Ferreira Lopes,⁴⁹ F. Ferreira Rodrigues,² S. Ferreres Sole,³² M. Ferrillo,⁵⁰ M. Ferro-Luzzi,⁴⁸ S. Filippov,⁴¹ R. A. Fini,¹⁹
 M. Fiorini,^{21,f} M. Firllej,³⁵ K. M. Fischer,⁶³ C. Fitzpatrick,⁶² T. Fiutowski,³⁵ F. Fleuret,¹² M. Fontana,¹³ F. Fontanelli,^{24,h}
 R. Forty,⁴⁸ V. Franco Lima,⁶⁰ M. Franco Sevilla,⁶⁶ M. Frank,⁴⁸ E. Franzoso,²¹ G. Frau,¹⁷ C. Frei,⁴⁸ D. A. Friday,⁵⁹ J. Fu,²⁶
 Q. Fuehring,¹⁵ W. Funk,⁴⁸ E. Gabriel,³² T. Gaintseva,⁴² A. Gallas Torreira,⁴⁶ D. Galli,^{20,d} S. Gambetta,^{58,48} Y. Gan,³
 M. Gandelman,² P. Gandini,²⁶ Y. Gao,⁴ M. Garau,²⁷ L. M. Garcia Martin,⁵⁶ P. Garcia Moreno,⁴⁵ J. García Pardiñas,²⁵
 B. Garcia Plana,⁴⁶ F. A. Garcia Rosales,¹² L. Garrido,⁴⁵ C. Gaspar,⁴⁸ R. E. Geertsema,³² D. Gerick,¹⁷ L. L. Gerken,¹⁵
 E. Gersabeck,⁶² M. Gersabeck,⁶² T. Gershon,⁵⁶ D. Gerstel,¹⁰ Ph. Ghez,⁸ V. Gibson,⁵⁵ M. Giovannetti,^{23,j} A. Gioventù,⁴⁶
 P. Gironella Gironell,⁴⁵ L. Giubega,³⁷ C. Giugliano,^{21,48,f} K. Gizdov,⁵⁸ E. L. Gkougkousis,⁴⁸ V. V. Gligorov,¹³ C. Göbel,⁷⁰
 E. Golobardes,⁸⁴ D. Golubkov,³⁹ A. Golutvin,^{61,81} A. Gomes,^{1,a} S. Gomez Fernandez,⁴⁵ F. Goncalves Abrantes,⁷⁰
 M. Goncerz,³⁴ G. Gong,³ P. Gorbounov,³⁹ I. V. Gorelov,⁴⁰ C. Gotti,^{25,i} E. Govorkova,⁴⁸ J. P. Grabowski,¹⁷
 R. Graciani Diaz,⁴⁵ T. Grammatico,¹³ L. A. Granado Cardoso,⁴⁸ E. Graugés,⁴⁵ E. Graverini,⁴⁹ G. Graziani,²² A. Greco,³⁷
 L. M. Greeven,³² P. Griffith,²¹ L. Grillo,⁶² S. Gromov,⁸¹ B. R. Gruberg Cazon,⁶³ C. Gu,³ M. Guarise,²¹ P. A. Günther,¹⁷
 E. Gushchin,⁴¹ A. Guth,¹⁴ Y. Guz,^{44,48} T. Gys,⁴⁸ T. Hadavizadeh,⁶⁹ G. Haefeli,⁴⁹ C. Haen,⁴⁸ J. Haimberger,⁴⁸
 T. Halewood-leagas,⁶⁰ P. M. Hamilton,⁶⁶ Q. Han,⁷ X. Han,¹⁷ T. H. Hancock,⁶³ S. Hansmann-Menzemer,¹⁷ N. Harnew,⁶³
 T. Harrison,⁶⁰ C. Hasse,⁴⁸ M. Hatch,⁴⁸ J. He,⁵ M. Hecker,⁶¹ K. Heijhoff,³² K. Heinicke,¹⁵ A. M. Hennequin,⁴⁸ K. Hennessy,⁶⁰
 L. Henry,^{26,47} J. Heuel,¹⁴ A. Hicheur,² D. Hill,⁴⁹ M. Hilton,⁶² S. E. Hollitt,¹⁵ J. Hu,¹⁷ J. Hu,⁷² W. Hu,⁷ W. Huang,⁵
 X. Huang,⁷³ W. Hulsbergen,³² R. J. Hunter,⁵⁶ M. Hushchyn,⁸² D. Hutchcroft,⁶⁰ D. Hynds,³² P. Ibis,¹⁵ M. Idzik,³⁵ D. Ilin,³⁸
 P. Ilten,⁶⁵ A. Inglessi,³⁸ A. Ishteev,⁸¹ K. Ivshin,³⁸ R. Jacobsson,⁴⁸ S. Jakobsen,⁴⁸ E. Jans,³² B. K. Jashal,⁴⁷ A. Jawahery,⁶⁶
 V. Jevtic,¹⁵ M. Jezabek,³⁴ F. Jiang,³ M. John,⁶³ D. Johnson,⁴⁸ C. R. Jones,⁵⁵ T. P. Jones,⁵⁶ B. Jost,⁴⁸ N. Jurik,⁴⁸ S. Kandybei,⁵¹
 Y. Kang,³ M. Karacson,⁴⁸ N. Kazeev,⁸² F. Keizer,^{55,48} M. Kenzie,⁵⁶ T. Ketel,³³ B. Khanji,¹⁵ A. Kharisova,⁸³ S. Kholodenko,⁴⁴
 K. E. Kim,⁶⁸ T. Kirn,¹⁴ V. S. Kirsebom,⁴⁹ O. Kitouni,⁶⁴ S. Klaver,³² K. Klimaszewski,³⁶ S. Koliiev,⁵² A. Kondybayeva,⁸¹
 A. Konoplyannikov,³⁹ P. Kopciwicz,³⁵ R. Kopečna,¹⁷ P. Koppenburg,³² M. Korolev,⁴⁰ I. Kostiuk,^{32,52} O. Kot,⁵²
 S. Kotriakhova,^{38,31} P. Kravchenko,³⁸ L. Kravchuk,⁴¹ R. D. Krawczyk,⁴⁸ M. Kreps,⁵⁶ F. Kress,⁶¹ S. Kretschmar,¹⁴
 P. Krokovny,^{43,u} W. Krupa,³⁵ W. Krzemien,³⁶ W. Kucewicz,^{34,k} M. Kucharczyk,³⁴ V. Kudryavtsev,^{43,u} H. S. Kuindersma,³²
 G. J. Kunde,⁶⁷ T. Kvaratskheliya,³⁹ D. Lacarrere,⁴⁸ G. Lafferty,⁶² A. Lai,²⁷ A. Lampis,²⁷ D. Lancierini,⁵⁰ J. J. Lane,⁶²
 R. Lane,⁵⁴ G. Lanfranchi,²³ C. Langenbruch,¹⁴ J. Langer,¹⁵ O. Lantwin,^{50,81} T. Latham,⁵⁶ F. Lazzari,^{29,s} R. Le Gac,¹⁰
 S. H. Lee,⁸⁵ R. Lefèvre,⁹ A. Leflat,⁴⁰ S. Legotin,⁸¹ O. Leroy,¹⁰ T. Lesiak,³⁴ B. Leverington,¹⁷ H. Li,⁷² L. Li,⁶³ P. Li,¹⁷ Y. Li,⁶
 Y. Li,⁶ Z. Li,⁶⁸ X. Liang,⁶⁸ T. Lin,⁶¹ R. Lindner,⁴⁸ V. Lisovskyi,¹⁵ R. Litvinov,²⁷ G. Liu,⁷² H. Liu,⁵ S. Liu,⁶ X. Liu,³ A. Loi,²⁷
 J. Lomba Castro,⁴⁶ I. Longstaff,⁵⁹ J. H. Lopes,² G. Loustau,⁵⁰ G. H. Lovell,⁵⁵ Y. Lu,⁶ D. Lucchesi,^{28,1} S. Luchuk,⁴¹
 M. Lucio Martinez,³² V. Lukashenko,³² Y. Luo,³ A. Lupato,⁶² E. Luppi,^{21,f} O. Lupton,⁵⁶ A. Lusiani,^{29,q} X. Lyu,⁵ L. Ma,⁶
 S. Maccolini,^{20,d} F. Machefert,¹¹ F. Maciuc,³⁷ V. Macko,⁴⁹ P. Mackowiak,¹⁵ S. Maddrell-Mander,⁵⁴ O. Madejczyk,³⁵
 L. R. Madhan Mohan,⁵⁴ O. Maev,³⁸ A. Maevskiy,⁸² D. Maisuzenko,³⁸ M. W. Majewski,³⁵ S. Malde,⁶³ B. Malecki,⁴⁸
 A. Malinin,⁸⁰ T. Maltsev,^{43,u} H. Malygina,¹⁷ G. Manca,^{27,e} G. Mancinelli,¹⁰ R. Manera Escalero,⁴⁵ D. Manuzzi,^{20,d}
 D. Marangotto,^{26,n} J. Maratas,^{9,t} J. F. Marchand,⁸ U. Marconi,²⁰ S. Mariani,^{22,48,g} C. Marin Benito,¹¹ M. Marinangeli,⁴⁹
 P. Marino,⁴⁹ J. Marks,¹⁷ P. J. Marshall,⁶⁰ G. Martellotti,³¹ L. Martinazzoli,^{48,i} M. Martinelli,^{25,i} D. Martinez Santos,⁴⁶
 F. Martinez Vidal,⁴⁷ A. Massafferri,¹ M. Materok,¹⁴ R. Matev,⁴⁸ A. Mathad,⁵⁰ Z. Mathe,⁴⁸ V. Matiunin,³⁹ C. Matteuzzi,²⁵
 K. R. Mattioli,⁸⁵ A. Mauri,³² E. Maurice,¹² J. Mauricio,⁴⁵ M. Mazurek,³⁶ M. McCann,⁶¹ L. McConnell,¹⁸ T. H. Mcgrath,⁶²
 A. McNab,⁶² R. McNulty,¹⁸ J. V. Mead,⁶⁰ B. Meadows,⁶⁵ C. Meaux,¹⁰ G. Meier,¹⁵ N. Meinert,⁷⁶ D. Melnychuk,³⁶
 S. Meloni,^{25,i} M. Merk,^{32,79} A. Merli,²⁶ L. Meyer Garcia,² M. Mikhasenko,⁴⁸ D. A. Milanes,⁷⁴ E. Millard,⁵⁶
 M. Milovanovic,⁴⁸ M.-N. Minard,⁸ L. Minzoni,^{21,f} S. E. Mitchell,⁵⁸ B. Mitreska,⁶² D. S. Mitzel,⁴⁸ A. Mödden,¹⁵
 R. A. Mohammed,⁶³ R. D. Moise,⁶¹ T. Mombächer,¹⁵ I. A. Monroy,⁷⁴ S. Monteil,⁹ M. Morandin,²⁸ G. Morello,²³
 M. J. Morello,^{29,q} J. Moron,³⁵ A. B. Morris,⁷⁵ A. G. Morris,⁵⁶ R. Mountain,⁶⁸ H. Mu,³ F. Muheim,⁵⁸ M. Mukherjee,⁷
 M. Mulder,⁴⁸ D. Müller,⁴⁸ K. Müller,⁵⁰ C. H. Murphy,⁶³ D. Murray,⁶² P. Muzzetto,^{27,48} P. Naik,⁵⁴ T. Nakada,⁴⁹
 R. Nandakumar,⁵⁷ T. Nanut,⁴⁹ I. Nasteva,² M. Needham,⁵⁸ I. Neri,^{21,f} N. Neri,^{26,n} S. Neubert,⁷⁵ N. Neufeld,⁴⁸
 R. Newcombe,⁶¹ T. D. Nguyen,⁴⁹ C. Nguyen-Mau,⁴⁹ E. M. Niel,¹¹ S. Nieswand,¹⁴ N. Nikitin,⁴⁰ N. S. Nolte,⁴⁸ C. Nunez,⁸⁵
 A. Oblakowska-Mucha,³⁵ V. Obraztsov,⁴⁴ D. P. O'Hanlon,⁵⁴ R. Oldeman,^{27,e} C. J. G. Onderwater,⁷⁸ A. Ossowska,³⁴
 J. M. Otalora Goicochea,² T. Ovsiannikova,³⁹ P. Owen,⁵⁰ A. Oyangueren,⁴⁷ B. Pagare,⁵⁶ P. R. Pais,⁴⁸ T. Pajero,^{29,48,q}
 A. Palano,¹⁹ M. Palutan,²³ Y. Pan,⁶² G. Panshin,⁸³ A. Papanestis,⁵⁷ M. Pappagallo,^{19,c} L. L. Pappalardo,^{21,f}
 C. Pappenheimer,⁶⁵ W. Parker,⁶⁶ C. Parkes,⁶² C. J. Parkinson,⁴⁶ B. Passalacqua,²¹ G. Passaleva,²² A. Pastore,¹⁹ M. Patel,⁶¹

C. Patrignani,^{20,d} C. J. Pawley,⁷⁹ A. Pearce,⁴⁸ A. Pellegrino,³² M. Pepe Altarelli,⁴⁸ S. Perazzini,²⁰ D. Pereima,³⁹ P. Perret,⁹ K. Petridis,⁵⁴ A. Petrolini,^{24,h} A. Petrov,⁸⁰ S. Petrucci,⁵⁸ M. Petruzzo,²⁶ A. Philippov,⁴² L. Pica,²⁹ M. Piccini,⁷⁷ B. Pietrzyk,⁸ G. Pietrzyk,⁴⁹ M. Pili,⁶³ D. Pinci,³¹ F. Pisani,⁴⁸ A. Piucci,¹⁷ Resmi P. K.,¹⁰ V. Placinta,³⁷ J. Plews,⁵³ M. Plo Casasus,⁴⁶ F. Polci,¹³ M. Poli Lener,²³ M. Poliakov,⁶⁸ A. Poluektov,¹⁰ N. Polukhina,^{81,b} I. Polyakov,⁶⁸ E. Polycarpo,² G. J. Pomery,⁵⁴ S. Ponce,⁴⁸ D. Popov,^{5,48} S. Popov,⁴² S. Poslavskii,⁴⁴ K. Prasad,³⁴ L. Promberger,⁴⁸ C. Prouve,⁴⁶ V. Pugatch,⁵² H. Pullen,⁶³ G. Punzi,^{29,m} W. Qian,⁵ J. Qin,⁵ R. Quagliani,¹³ B. Quintana,⁸ N. V. Raab,¹⁸ R. I. Rabadan Trejo,¹⁰ B. Rachwal,³⁵ J. H. Rademacker,⁵⁴ M. Rama,²⁹ M. Ramos Pernas,⁵⁶ M. S. Rangel,² F. Ratnikov,^{42,82} G. Raven,³³ M. Reboud,⁸ F. Redi,⁴⁹ F. Reiss,¹³ C. Remon Alepuz,⁴⁷ Z. Ren,³ V. Renaudin,⁶³ R. Ribatti,²⁹ S. Ricciardi,⁵⁷ D. S. Richards,⁵⁷ K. Rinnert,⁶⁰ P. Robbe,¹¹ A. Robert,¹³ G. Robertson,⁵⁸ A. B. Rodrigues,⁴⁹ E. Rodrigues,⁶⁰ J. A. Rodriguez Lopez,⁷⁴ A. Rollings,⁶³ P. Roloff,⁴⁸ V. Romanovskiy,⁴⁴ M. Romero Lamas,⁴⁶ A. Romero Vidal,⁴⁶ J. D. Roth,⁸⁵ M. Rotondo,²³ M. S. Rudolph,⁶⁸ T. Ruf,⁴⁸ J. Ruiz Vidal,⁴⁷ A. Ryzhikov,⁸² J. Ryzka,³⁵ J. J. Saborido Silva,⁴⁶ N. Sagidova,³⁸ N. Sahoo,⁵⁶ B. Saitta,^{27,e} D. Sanchez Gonzalo,⁴⁵ C. Sanchez Gras,³² R. Santacesaria,³¹ C. Santamarina Rios,⁴⁶ M. Santimaria,²³ E. Santovetti,^{30,j} D. Saranin,⁸¹ G. Sarpis,⁵⁹ M. Sarpis,⁷⁵ A. Sarti,³¹ C. Satriano,^{31,p} A. Satta,³⁰ M. Saur,⁵ D. Savrina,^{39,40} H. Sazak,⁹ L. G. Scantlebury Smead,⁶³ S. Schael,¹⁴ M. Schellenberg,¹⁵ M. Schiller,⁵⁹ H. Schindler,⁴⁸ M. Schmelling,¹⁶ B. Schmidt,⁴⁸ O. Schneider,⁴⁹ A. Schopper,⁴⁸ M. Schubiger,³² S. Schulte,⁴⁹ M. H. Schune,¹¹ R. Schwemmer,⁴⁸ B. Sciascia,²³ A. Sciubba,³¹ S. Sellam,⁴⁶ A. Semennikov,³⁹ M. Senghi Soares,³³ A. Sergi,^{53,48} N. Serra,⁵⁰ L. Sestini,²⁸ A. Seuthe,¹⁵ P. Seyfert,⁴⁸ D. M. Shangase,⁸⁵ M. Shapkin,⁴⁴ I. Shchemerov,⁸¹ L. Shchutska,⁴⁹ T. Shears,⁶⁰ L. Shekhtman,^{43,u} Z. Shen,⁴ V. Shevchenko,⁸⁰ E. B. Shields,^{25,i} E. Shmanin,⁸¹ J. D. Shupperd,⁶⁸ B. G. Siddi,²¹ R. Silva Coutinho,⁵⁰ G. Simi,²⁸ S. Simone,^{19,c} I. Skiba,^{21,f} N. Skidmore,⁶² T. Skwarnicki,⁶⁸ M. W. Slater,⁵³ J. C. Smallwood,⁶³ J. G. Smeaton,⁵⁵ A. Smetkina,³⁹ E. Smith,¹⁴ M. Smith,⁶¹ A. Snoch,³² M. Soares,²⁰ L. Soares Lavra,⁹ M. D. Sokoloff,⁶⁵ F. J. P. Soler,⁵⁹ A. Solovov,³⁸ I. Solovyev,³⁸ F. L. Souza De Almeida,² B. Souza De Paula,² B. Spaan,¹⁵ E. Spadaro Norella,^{26,n} P. Spradlin,⁵⁹ F. Stagni,⁴⁸ M. Stahl,⁶⁵ S. Stahl,⁴⁸ P. Stefko,⁴⁹ O. Steinkamp,^{50,81} S. Stemmler,¹⁷ O. Stenyakin,⁴⁴ H. Stevens,¹⁵ S. Stone,⁶⁸ M. E. Stramaglia,⁴⁹ M. Straticiu,³⁷ D. Strelakina,⁸¹ S. Strovk,⁸³ F. Suljik,⁶³ J. Sun,²⁷ L. Sun,⁷³ Y. Sun,⁶⁶ P. Sviha,⁶² P. N. Swallow,⁵³ K. Swientek,³⁵ A. Szabelski,³⁶ T. Szumlak,³⁵ M. Szymanski,⁴⁸ S. Taneja,⁶² F. Teubert,⁴⁸ E. Thomas,⁴⁸ K. A. Thomson,⁶⁰ M. J. Tilley,⁶¹ V. Tisserand,⁹ S. T'Jampens,⁸ M. Tobin,⁶ S. Tolch,⁴⁸ L. Tomassetti,^{21,f} D. Torres Machado,¹ D. Y. Tou,¹³ M. Traill,⁵⁹ M. T. Tran,⁴⁹ E. Trifonova,⁸¹ C. Trippl,⁴⁹ G. Tuci,^{29,m} A. Tully,⁴⁹ N. Tuning,³² A. Ukleja,³⁶ D. J. Unverzagt,¹⁷ A. Usachov,³² A. Ustyuzhanin,^{42,82} U. Uwer,¹⁷ A. Vagner,⁸³ V. Vagnoni,²⁰ A. Valassi,⁴⁸ G. Valenti,²⁰ N. Valls Canudas,⁴⁵ M. van Beuzekom,³² E. van Herwijnen,⁸¹ C. B. Van Hulse,¹⁸ M. van Veghel,⁷⁸ R. Vazquez Gomez,⁴⁶ P. Vazquez Regueiro,⁴⁶ C. Vázquez Sierra,⁴⁸ S. Vecchi,²¹ J. J. Velthuis,⁵⁴ M. Veltri,^{22,o} A. Venkateswaran,⁶⁸ M. Veronesi,³² M. Vesterinen,⁵⁶ D. Vieira,⁶⁵ M. Vieites Diaz,⁴⁹ H. Viemann,⁷⁶ X. Vilasis-Cardona,⁸⁴ E. Vilella Figueras,⁶⁰ P. Vincent,¹³ G. Vitali,²⁹ A. Vollhardt,⁵⁰ D. Vom Bruch,¹³ A. Vorobyev,³⁸ V. Vorobyev,^{43,u} N. Voropaev,³⁸ R. Waldi,⁷⁶ J. Walsh,²⁹ C. Wang,¹⁷ J. Wang,³ J. Wang,⁷³ J. Wang,⁴ J. Wang,⁶ M. Wang,³ R. Wang,⁵⁴ Y. Wang,⁷ Z. Wang,⁵⁰ H. M. Wark,⁶⁰ N. K. Watson,⁵³ S. G. Weber,¹³ D. Websdale,⁶¹ C. Weissler,⁶⁴ B. D. C. Westhenry,⁵⁴ D. J. White,⁶² M. Whitehead,⁵⁴ D. Wiedner,¹⁵ G. Wilkinson,⁶³ M. Wilkinson,⁶⁸ I. Williams,⁵⁵ M. Williams,^{64,69} M. R. J. Williams,⁵⁸ F. F. Wilson,⁵⁷ W. Wislicki,³⁶ M. Witek,³⁴ L. Witola,¹⁷ G. Wormser,¹¹ S. A. Wotton,⁵⁵ H. Wu,⁶⁸ K. Wyllie,⁴⁸ Z. Xiang,⁵ D. Xiao,⁷ Y. Xie,⁷ A. Xu,⁴ J. Xu,⁵ L. Xu,³ M. Xu,⁷ Q. Xu,⁵ Z. Xu,⁵ Z. Xu,⁴ D. Yang,³ Y. Yang,⁵ Z. Yang,³ Z. Yang,⁶⁶ Y. Yao,⁶⁸ L. E. Yeomans,⁶⁰ H. Yin,⁷ J. Yu,⁷¹ X. Yuan,⁶⁸ O. Yushchenko,⁴⁴ K. A. Zarebski,⁵³ M. Zavertyaev,^{16,b} M. Zdybal,³⁴ O. Zenaiev,⁴⁸ M. Zeng,³ D. Zhang,⁷ L. Zhang,³ S. Zhang,⁴ Y. Zhang,⁴ Y. Zhang,⁶³ A. Zhelezov,¹⁷ Y. Zheng,⁵ X. Zhou,⁵ Y. Zhou,⁵ X. Zhu,³ V. Zhukov,^{14,40} J. B. Zonneveld,⁵⁸ S. Zucchelli,^{20,d} D. Zuliani,²⁸ and G. Zunica⁶²

(LHCb Collaboration)

¹Centro Brasileiro de Pesquisas Físicas (CBPF), Rio de Janeiro, Brazil²Universidade Federal do Rio de Janeiro (UFRJ), Rio de Janeiro, Brazil³Center for High Energy Physics, Tsinghua University, Beijing, China⁴School of Physics State Key Laboratory of Nuclear Physics and Technology, Peking University, Beijing, China⁵University of Chinese Academy of Sciences, Beijing, China⁶Institute Of High Energy Physics (IHEP), Beijing, China⁷Institute of Particle Physics, Central China Normal University, Wuhan, Hubei, China⁸Univ. Grenoble Alpes, Univ. Savoie Mont Blanc, CNRS, IN2P3-LAPP, Annecy, France

- ⁹Université Clermont Auvergne, CNRS/IN2P3, LPC, Clermont-Ferrand, France
- ¹⁰Aix Marseille Univ, CNRS/IN2P3, CPPM, Marseille, France
- ¹¹Université Paris-Saclay, CNRS/IN2P3, IJCLab, Orsay, France
- ¹²Laboratoire Leprince-ringuet (llr), Palaiseau, France
- ¹³LPNHE, Sorbonne Université, Paris Diderot Sorbonne Paris Cité, CNRS/IN2P3, Paris, France
- ¹⁴I. Physikalisches Institut, RWTH Aachen University, Aachen, Germany
- ¹⁵Fakultät Physik, Technische Universität Dortmund, Dortmund, Germany
- ¹⁶Max-Planck-Institut für Kernphysik (MPIK), Heidelberg, Germany
- ¹⁷Physikalisches Institut, Ruprecht-Karls-Universität Heidelberg, Heidelberg, Germany
- ¹⁸School of Physics, University College Dublin, Dublin, Ireland
- ¹⁹INFN Sezione di Bari, Bari, Italy
- ²⁰INFN Sezione di Bologna, Bologna, Italy
- ²¹INFN Sezione di Ferrara, Ferrara, Italy
- ²²INFN Sezione di Firenze, Firenze, Italy
- ²³INFN Laboratori Nazionali di Frascati, Frascati, Italy
- ²⁴INFN Sezione di Genova, Genova, Italy
- ²⁵INFN Sezione di Milano-Bicocca, Milano, Italy
- ²⁶INFN Sezione di Milano, Milano, Italy
- ²⁷INFN Sezione di Cagliari, Monserrato, Italy
- ²⁸Università degli Studi di Padova, Università e INFN, Padova, Padova, Italy
- ²⁹INFN Sezione di Pisa, Pisa, Italy
- ³⁰INFN Sezione di Roma Tor Vergata, Roma, Italy
- ³¹INFN Sezione di Roma La Sapienza, Roma, Italy
- ³²Nikhef National Institute for Subatomic Physics, Amsterdam, Netherlands
- ³³Nikhef National Institute for Subatomic Physics and VU University Amsterdam, Amsterdam, Netherlands
- ³⁴Henryk Niewodniczanski Institute of Nuclear Physics Polish Academy of Sciences, Kraków, Poland
- ³⁵AGH—University of Science and Technology, Faculty of Physics and Applied Computer Science, Kraków, Poland
- ³⁶National Center for Nuclear Research (NCBJ), Warsaw, Poland
- ³⁷Horia Hulubei National Institute of Physics and Nuclear Engineering, Bucharest-Magurele, Romania
- ³⁸Petersburg Nuclear Physics Institute NRC Kurchatov Institute (PNPI NRC KI), Gatchina, Russia
- ³⁹Institute of Theoretical and Experimental Physics NRC Kurchatov Institute (ITEP NRC KI), Moscow, Russia
- ⁴⁰Institute of Nuclear Physics, Moscow State University (SINP MSU), Moscow, Russia
- ⁴¹Institute for Nuclear Research of the Russian Academy of Sciences (INR RAS), Moscow, Russia
- ⁴²Yandex School of Data Analysis, Moscow, Russia
- ⁴³Budker Institute of Nuclear Physics (SB RAS), Novosibirsk, Russia
- ⁴⁴Institute for High Energy Physics NRC Kurchatov Institute (IHEP NRC KI), Protvino, Russia, Protvino, Russia
- ⁴⁵ICCUB, Universitat de Barcelona, Barcelona, Spain
- ⁴⁶Instituto Galego de Física de Altas Enerxías (IGFAE), Universidade de Santiago de Compostela, Santiago de Compostela, Spain
- ⁴⁷Instituto de Física Corpuscular, Centro Mixto Universidad de Valencia—CSIC, Valencia, Spain
- ⁴⁸European Organization for Nuclear Research (CERN), Geneva, Switzerland
- ⁴⁹Institute of Physics, Ecole Polytechnique Fédérale de Lausanne (EPFL), Lausanne, Switzerland
- ⁵⁰Physik-Institut, Universität Zürich, Zürich, Switzerland
- ⁵¹NSC Kharkiv Institute of Physics and Technology (NSC KIPT), Kharkiv, Ukraine
- ⁵²Institute for Nuclear Research of the National Academy of Sciences (KINR), Kyiv, Ukraine
- ⁵³University of Birmingham, Birmingham, United Kingdom
- ⁵⁴H.H. Wills Physics Laboratory, University of Bristol, Bristol, United Kingdom
- ⁵⁵Cavendish Laboratory, University of Cambridge, Cambridge, United Kingdom
- ⁵⁶Department of Physics, University of Warwick, Coventry, United Kingdom
- ⁵⁷STFC Rutherford Appleton Laboratory, Didcot, United Kingdom
- ⁵⁸School of Physics and Astronomy, University of Edinburgh, Edinburgh, United Kingdom
- ⁵⁹School of Physics and Astronomy, University of Glasgow, Glasgow, United Kingdom
- ⁶⁰Oliver Lodge Laboratory, University of Liverpool, Liverpool, United Kingdom
- ⁶¹Imperial College London, London, United Kingdom
- ⁶²Department of Physics and Astronomy, University of Manchester, Manchester, United Kingdom
- ⁶³Department of Physics, University of Oxford, Oxford, United Kingdom
- ⁶⁴Massachusetts Institute of Technology, Cambridge, Massachusetts, USA
- ⁶⁵University of Cincinnati, Cincinnati, Ohio, USA
- ⁶⁶University of Maryland, College Park, Maryland, USA
- ⁶⁷Los Alamos National Laboratory (LANL), Los Alamos, New Mexico, USA
- ⁶⁸Syracuse University, Syracuse, New York, USA

⁶⁹*School of Physics and Astronomy, Monash University, Melbourne, Australia
(associated with Department of Physics, University of Warwick, Coventry, United Kingdom)*

⁷⁰*Pontifícia Universidade Católica do Rio de Janeiro (PUC-Rio), Rio de Janeiro, Brazil
(associated with Universidade Federal do Rio de Janeiro (UFRJ), Rio de Janeiro, Brazil)*

⁷¹*Physics and Micro Electronic College, Hunan University, Changsha City, China
(associated with Institute of Particle Physics, Central China Normal University, Wuhan, Hubei, China)*

⁷²*Guangdong Provincial Key Laboratory of Nuclear Science, Institute of Quantum Matter, South China Normal University,
Guangzhou, China*

(associated with Center for High Energy Physics, Tsinghua University, Beijing, China)

⁷³*School of Physics and Technology, Wuhan University, Wuhan, China
(associated with Center for High Energy Physics, Tsinghua University, Beijing, China)*

⁷⁴*Departamento de Física, Universidad Nacional de Colombia, Bogota, Colombia
(associated with LPNHE, Sorbonne Université, Paris Diderot Sorbonne Paris Cité, CNRS/IN2P3, Paris, France)*

⁷⁵*Universität Bonn—Helmholtz-Institut für Strahlen und Kernphysik, Bonn, Germany
(associated with Physikalisches Institut, Ruprecht-Karls-Universität Heidelberg, Heidelberg, Germany)*

⁷⁶*Institut für Physik, Universität Rostock, Rostock, Germany
(associated with Physikalisches Institut, Ruprecht-Karls-Universität Heidelberg, Heidelberg, Germany)*

⁷⁷*INFN Sezione di Perugia, Perugia, Italy
(associated with INFN Sezione di Ferrara, Ferrara, Italy)*

⁷⁸*Van Swinderen Institute, University of Groningen, Groningen, Netherlands
(associated with Nikhef National Institute for Subatomic Physics, Amsterdam, Netherlands)*

⁷⁹*Universiteit Maastricht, Maastricht, Netherlands
(associated with Nikhef National Institute for Subatomic Physics, Amsterdam, Netherlands)*

⁸⁰*National Research Centre Kurchatov Institute, Moscow, Russia
(associated with Institute of Theoretical and Experimental Physics NRC Kurchatov Institute (ITEP NRC KI), Moscow, Russia)*

⁸¹*National University of Science and Technology “MISIS”, Moscow, Russia
(associated with Institute of Theoretical and Experimental Physics NRC Kurchatov Institute (ITEP NRC KI), Moscow, Russia)*

⁸²*National Research University Higher School of Economics, Moscow, Russia
(associated with Yandex School of Data Analysis, Moscow, Russia)*

⁸³*National Research Tomsk Polytechnic University, Tomsk, Russia
(associated with Institute of Theoretical and Experimental Physics NRC Kurchatov Institute (ITEP NRC KI), Moscow, Russia)*

⁸⁴*DS4DS, La Salle, Universitat Ramon Llull, Barcelona, Spain
(associated with ICCUB, Universitat de Barcelona, Barcelona, Spain)*

⁸⁵*University of Michigan, Ann Arbor, Michigan, USA
(associated with Syracuse University, Syracuse, New York, USA)*

^aAlso at Universidade Federal do Triângulo Mineiro (UFTM), Uberaba-MG, Brazil.

^bAlso at P.N. Lebedev Physical Institute, Russian Academy of Science (LPI RAS), Moscow, Russia.

^cAlso at Università di Bari, Bari, Italy.

^dAlso at Università di Bologna, Bologna, Italy.

^eAlso at Università di Cagliari, Cagliari, Italy.

^fAlso at Università di Ferrara, Ferrara, Italy.

^gAlso at Università di Firenze, Firenze, Italy.

^hAlso at Università di Genova, Genova, Italy.

ⁱAlso at Università di Milano Bicocca, Milano, Italy.

^jAlso at Università di Roma Tor Vergata, Roma, Italy.

^kAlso at AGH—University of Science and Technology, Faculty of Computer Science, Electronics and Telecommunications, Kraków, Poland.

^lAlso at Università di Padova, Padova, Italy.

^mAlso at Università di Pisa, Pisa, Italy.

ⁿAlso at Università degli Studi di Milano, Milano, Italy.

^oAlso at Università di Urbino, Urbino, Italy.

^pAlso at Università della Basilicata, Potenza, Italy.

^qAlso at Scuola Normale Superiore, Pisa, Italy.

^rAlso at Università di Modena e Reggio Emilia, Modena, Italy.

^sAlso at Università di Siena, Siena, Italy.

^tAlso at MSU—Iligan Institute of Technology (MSU-IIT), Iligan, Philippines.

^uAlso at Novosibirsk State University, Novosibirsk, Russia.

^vAlso at Department of Physics and Astronomy, Uppsala University, Uppsala, Sweden.